Fluid substitution effects on seismic anisotropy

Long Huang, Robert R. Stewart, Nikolay Dyaur, University of Houston and Samik Sil, ConocoPhillips*

SUMMARY

We derive specific equations for orthorhombic media to analyze fluid substitution effects in porous fractured rocks. We assess the influence of fluid substitution (from gas to brine), on elastic moduli, velocities, anisotropy, and azimuthal amplitude variation. We find that in the direction normal to fractures, P-wave modulus increases as much as 56% and P-wave velocity increases up to 19% for brine substitution. For the direction parallel to fractures, P-wave velocity almost remains constant when porosity is low (5%), but can increase up to 4% if porosity if high (25%). Since P-waves in two different directions have different sensitivities to fluids and fractures, the Thomsen's parameters (defined for orthorhombic symmetry), $\varepsilon^{1,2}$ and $\delta^{1,2}$, are sensitive to fluid types and fractures. We also found that $\delta^{1,2}$ is sensitive to porosity for liquid-saturation, but insensitive to porosity for the case of gas-saturation. Gassmann assumes (and as has been observed) that shear modulus does not depend on fluids. And we observe no changes in shear-wave splitting ($\gamma^{1,2}$) for different fluids. The azimuthal amplitude variation as the result of anisotropy contrast between the interfaces, is dependent on fluid type, fractures and porosity. We observe up to 12% increase in azimuthal amplitude variation for low porosity sands after brine saturation, and 6% decrease for high porosity sands. The equations we have derived are straight forward to understand and provide us a useful tool as to quantitatively evaluate the effects of fluid substitution on seismic anisotropy.

INTRODUCTION

Understanding the effects of fluid substitution in seismic signal is a key aspect of subsurface exploration and production. A commonly used method for fluid substitution comes from the work of Gassmann (1951), which relates the bulk modulus of a rock to its porosity, rock matrix, and fluid properties. The isotropic Gassmann's equations are often used to assess the fluid substitution effects on rocks. Less well-known is that Gassmann (1951) also published a general equation for fluid substitution in anisotropic media, which can be used to evaluate fluid substitution effects on seismic anisotropy. His results can be written in terms of stiffness tensors, C_{ijkl}, where a repeated index implies a sum over 1-3 (Mavko and Bandyopadhyay, 2009):

$$C^{sat}_{ijkl} = C_{ijkl} + \frac{(K_m\delta_{ij} - C_{ij\alpha\alpha}/3)(K_m\delta_{ij} - C_{\beta\beta kl}/3)}{(K_m/K_{fl})\phi(K_m - K_{fl}) + (K_m - C_{ppqq}/9)}, \quad (1)$$

where,

$$\delta_{ij} = \begin{cases} 1, & \text{i = j} \\ 0, & \text{i} \neq \text{j} \end{cases}, \quad (2)$$

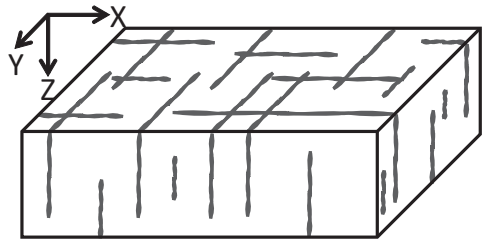

Figure 1. Schematic diagram of an orthorhombic (two orthogonal sets of vertical fractures in an isotropic background) medium.

$$C_{ppqq} = \sum_{p=1}^{3}\sum_{q=1}^{3} C_{ppqq}, \quad (3)$$

$$C_{ij\alpha\alpha} = \sum_{i=1}^{3}\sum_{j=1}^{3}\sum_{\alpha=1}^{3} C_{ij\alpha\alpha}, \quad (4)$$

From Equation 1, we need to know all the stiffness values of the rock if we want to use this equation. We seldom have enough measurements to do so. In this case, these equations become less useful and other methods to parameterise these equations are proposed. Gurevich (2003) and Sil et al. (2011) derived the anisotropic Gassmann's equations for an HTI rock based on a linear-slip model (Hsu and Schoenberg, 1993; Schoenberg and Sayers, 1995) and analyzed the effect of changing porosity and water saturation. The linear slip theory is free of crack geometry and it's an effective model of fractured media with parallel infinite fractures (Schoenberg, 1980, 1983). However, the equations they gave are again challenging to understand intuitively. Huang et al. (2013) recast Gurevich's equations in a manner easier to understand for an HTI medium. In this study, we extend the fluid substitution equations for orthorhombic media using the same theories and methods. Then, by using these new equations, numerical tests with sandstones are performed to compare the effects of porosity, fracture weakness on the P- and S-wave moduli and velocities, anisotropic parameters and azimuthal amplitude variations.

THEORY

We consider rocks with isotropic backgrounds with two orthogonal sets of vertical, parallel, rotationally invariant fractures (Bakulin et al., 2000), making it an orthorhombic medium. For the cases we consider here, we assume porous isotropic dry host rocks with interconnected pores and vertical fracture sets which contribute no or negligible porosity to the rocks. We saturate such rocks and predict the fluid effects on the rocks. For an orthorhombic medium with two vertical fracture sets (Figure 1), Bakulin et al. (2000) derived the effective stiffness matrix using linear slip theory (Equation 5 to 20).

$$C_{ij} = \begin{pmatrix} C_{11} & C_{12} & C_{13} & 0 & 0 & 0 \\ C_{12} & C_{22} & C_{23} & 0 & 0 & 0 \\ C_{13} & C_{23} & C_{33} & 0 & 0 & 0 \\ 0 & 0 & 0 & C_{44} & 0 & 0 \\ 0 & 0 & 0 & 0 & C_{55} & 0 \\ 0 & 0 & 0 & 0 & 0 & C_{66} \end{pmatrix} = \left(\begin{array}{c|c} \mathbf{C_1} & \mathbf{0} \\ \hline \mathbf{0} & \mathbf{C_2} \end{array}\right) \tag{5}$$

where $\mathbf{0}$ is the 3×3 zero matrix and $\mathbf{C_1}$ and $\mathbf{C_2}$ are given by

$$\mathbf{C_1} = \frac{1}{d}\begin{pmatrix} Ml_1m_3 & \lambda l_1m_1 & \lambda l_1m_2 \\ \lambda l_1m_1 & Ml_3m_1 & \lambda l_2m_1 \\ \lambda l_1m_2 & \lambda l_2m_1 & M(l_3m_3 - l_4) \end{pmatrix} \tag{6}$$

and

$$\mathbf{C_2} = \begin{pmatrix} \mu(1-\Delta_{T2}) & 0 & 0 \\ 0 & \mu(1-\Delta_{T1}) & 0 \\ 0 & 0 & \mu\frac{(1-\Delta_{T1})(1-\Delta_{T2})}{(1-\Delta_{T1}\Delta_{T2})} \end{pmatrix} \tag{7}$$

where,

$$M = \lambda + 2\mu, \tag{8}$$

$$r = \lambda/(\lambda+2\mu), \tag{9}$$

$$l_1 = 1-\Delta_{N1} \tag{10}$$

$$l_2 = 1-r\Delta_{N1} \tag{11}$$

$$l_3 = 1-r^2\Delta_{N1} \tag{12}$$

$$l_4 = 4r^2g^2\Delta_{N1}\Delta_N 2 \tag{13}$$

$$m_1 = 1-\Delta_{N2} \tag{14}$$

$$m_2 = 1-r\Delta_{N2} \tag{15}$$

$$m_3 = 1-r^2\Delta_{N2} \tag{16}$$

$$g = \mu/(\lambda+2\mu) = V_s^2/V_p^2 \tag{17}$$

$$d = 1-r^2\Delta_{N1}\Delta_{N2} \tag{18}$$

$$\Delta_{Ni} = Z_{Ni}M/(1+Z_{Ni}M) \tag{19}$$

$$\Delta_{Ti} = Z_{Ti}\mu/(1+Z_{Ti}\mu) \tag{20}$$

In the equations above, Δ_{Ni} and Δ_{Ti} (i=1,2) are the normal and tangential fracture weakness (defined in the same way as the HTI case) of the anisotropic fractured rocks. With the effective stiffness matrix of the dry rock, we can derive the expressions for $C_{1\alpha}$ and C_{pq}, and substitute them into equation 1, to get the explicit expressions for orthorhombic Gassmann's equations. Using equations above, we can express the following quantities (second-order terms are dropped) as

$$C_{1\alpha} = 3K(1-\Delta_{N1}-r\Delta_{N2}) \tag{21}$$

$$C_{2\alpha} = 3K(1-r\Delta_{N1}-\Delta_{N2}) \tag{22}$$

$$C_{3\alpha} = 3K(1-r\Delta_{N1}-r\Delta_{N2}) \tag{23}$$

$$C_{4\alpha} = C_{5\alpha} = C_{6\alpha} = 0 \tag{24}$$

$$C_{pq} = 9K(1-\frac{K(\Delta_{N1}+\Delta_{N2})}{\lambda+2\mu}) \tag{25}$$

By substituting the above equations into each C_{ij}^{sat}, we get the orthorhombic fluid substitution equations (Equation 26 to 31).

$$C_{11}^{sat} = M(1-\Delta_{N1}-r^2\Delta_{N2}) + \frac{(K_m - K(1-\Delta_{N1}-r\Delta_{N2}))^2}{(K_m/K_{fl})\phi(K_m-K_{fl}) + K_m - K + K^2(\Delta_{N1}+\Delta_{N2})/M} \tag{26}$$

$$C_{22}^{sat} = M(1-r^2\Delta_{N1}-\Delta_{N2}) + \frac{(K_m - K(1-r\Delta_{N1}-\Delta_{N2}))^2}{(K_m/K_{fl})\phi(K_m-K_{fl}) + K_m - K + K^2(\Delta_{N1}+\Delta_{N2})/M} \tag{27}$$

$$C_{33}^{sat} = M(1-r^2\Delta_{N1}-r^2\Delta_{N2}) + \frac{(K_m - K(1-r\Delta_{N1}-r\Delta_{N2}))^2}{(K_m/K_{fl})\phi(K_m-K_{fl}) + K_m - K + K^2(\Delta_{N1}+\Delta_{N2})/M} \tag{28}$$

$$C_{44}^{sat} = \mu(1-\Delta_{T2}) \tag{29}$$

$$C_{55}^{sat} = \mu(1-\Delta_{T1}) \tag{30}$$

$$C_{66}^{sat} = \mu\frac{(1-\Delta_{T1})(1-\Delta_{T2})}{(1-\Delta_{T1}\Delta_{T2})} \tag{31}$$

By using equation 26 to 31, we can perform anisotropic fluid substitution analysis for an orthorhombic medium.

ANALYSIS AND DISCUSSION

Since the equations are based on Gassmann's equations and linear slip theory, several assumptions should be satisfied: 1) All the pores that contribute the porosity in our equations are interconnected; 2) The fluid diffusion length is larger than the fracture size and spacing (Gurevich, 2003) which means low frequencies; 3) The background porous mineral matrix is isotropic; 4) the fracture systems contribute no or negligible porosity to the rocks.

Directly from the equations, we know that Gassmann's theory considers shear rigidity as independent of fluid type. This assumption is usually valid and people use it to predict shear-wave response to fluid infill in seismic exploration. O'Connell and Budiansky (1977) proposed that, for an isotropic material under undrained conditions, the shear modulus is the same as for dry conditions. Their results were confirmed by Hudson (2000). Recently, Thomsen (2012) derives similar results about shear wave dependence on fluid and concludes that the shear anisotropic parameter, γ, is independent of fluid content. However, high frequency (Zhang, 2010), pressure change (Tod, 2002), viscous fluid (Kato, 2010) and chemical reactions between rock frame and fluid, will lead to the shear-wave variation with fluid content. These are special cases when Gassmann's conditions are not satisfied. In fact, the fracture weakness (Δ_N) is a direct hydrocarbon indicator as it is sensitive to fluid (Schoenberg and Douma, 1988). For liquid-filled

rocks, Δ_N is almost 0. For gas-filled rocks, Δ_N almost equals to Δ_T. A source of error comes when we ignore the second-order terms of fracture weakness. This approximation works well when the fracture weakness is much less than 1. However, if the fracture weakness is large, this approximation will introduce errors and the predictions from the equations will collapse.

Our goal in this study is to analyze the fluid substitution effects on fractured rocks. We start with gas-saturated sandstones with 5% porosity and two fracture sets (characterized as $\Delta_{T1} = 0.1, \Delta_{T2} = 0.5$), then substitute gas for brine and oil and calculate the changes in elastic properties and anisotropy. The process is repeated as we increase porosity (from 5% to 25%). The effect of fluid substitution is directly calculated through the equations we have just derived. As for the influence of porosity, we consider only the background isotropic rock porosity. The influence of porosity is measured through the modeling of varying the porosity of background sandstone matrix. The background matrix properties are calculated using Krief's relations (Krief et al., 1990) for sandstones. The tangential fracture weakness (Δ_T) is a measure of fracture density and invariant to fluid type. The corresponding normal fracture weakness (Δ_N) for the dry model is calculated through (Sayers and Kachanov, 1995; Sil, 2013) respectively for both fracture sets:

$$\Delta_N = \frac{(2 - \nu + \nu\Delta_T)\Delta_T}{2}, \tag{32}$$

where ν is the Poisson's ration of the background rock. In this case, the tangential fracture weakness is only related to Poisson's ratio when it's dry. When the rocks are saturated with other fluid, Δ_N will change because it's dependent on fluid type. And the Gassmann's equations can be used as a measurement of the fluid effects on Δ_N as well.

We also study the fluid effects on the anisotropic parameters and azimuthal reflection coefficients. For orthorhombic media, the anisotropic parameters (known as the extended Thomsen's parameter, $\varepsilon^1, \delta^1, \gamma^1, \varepsilon^2, \delta^2, \gamma^2, \delta^3$) follow the definition of Tsvankin (1997). We introduce a top shale layer over the fractured sand reservoir to model the AVAZ effects. Here, we use the Mesaverde shale properties from Thomsen (1986). The shale layer has a vertical P-wave velocity of 4.359 km/s, vertical S-wave velocity of 3.048 km/s and a density of 2.81 g/cc. Its anisotropy is defined by the Thomsen's parameters as $\varepsilon = 0.172$, $\delta = 0$, and $\gamma = 0.157$. We do not consider any changes for the shale layer properties. We calculate the fluid properties of gas, brine and oil for a 3 km depth in the Gulf of Mexico for the modeling in the sandstone reservoir. The pore fluid properties are calculated through (Batzle and Wang, 1992) and implemented through the CREWES Fluid Property Calculator. We use the equations from Vavrycuk and Psenck (1998) which calculates the reflection coefficients for arbitrary elastic symmetry. For the measurement of azimuthal amplitude variation, we define an azimuthal-amplitude-variation factor, $AF(\theta)$, as a simple measurement of maximum azimuthal amplitude difference for the same incidence angle(θ).

$$AF(\theta) = R_{PP}^{max}(\theta) - R_{PP}^{min}(\theta); \tag{33}$$

porosity(ϕ)	ΔC_{11}	ΔC_{22}	ΔC_{33}
5%	38%	4%	2%
25%	56%	23%	19%
	ΔV_{PX}	ΔV_{PY}	ΔV_{PZ}
5%	16%	1%	0%
25%	18%	6%	4%
	$\Delta\varepsilon^1$	$\Delta\delta^1$	$\Delta\varepsilon^2$
5%	-22%	-9%	-35%
25%	-30%	-20%	-31%
	$\Delta\delta^2$	γ	$\Delta AF(30^\circ)$
5%	-5%	0%	12%
25%	-13%	0%	-6%

Table 1. Summary of influence of fluid substitution from gas to brine on sandstones with different porosity. Changes are measured in magnitude on acoustic moduli and velocities, anisotropy and azimuthal amplitude variations.

With the above modeling and equations, we perform three experiments as varying pore fluid, porosity, and investigate their influence on elastic moduli and velocities, anisotropic parameters and azimuthal amplitude variation for both HTI and orthorhombic media.

Table 1 shows the influence of fluid substitution from gas to brine on sandstones with different porosity. For low porosity sands after brine substitution, C_{11} increases 38%, C_{22} increases about 4% and C_{33} increases about 2%. We observe 16% increase in P-wave velocity in the direction normal to the "strong" fracture planes and subtle (or no) variations (1% and 0% increase respectively) are observed in the Y (normal to weak fracture planes) and Z (parallel to both fracture planes) directions. Shear-wave velocities decrease about 1% as the direct result of density change. Two sets of Thomsen-style parameters Tsvankin (1997) are defined based on the analogy between TI and orthorhombic media. Again, no changes in γ are expected. ε^1 and δ^1 characterise the P- and SV-wave in the YZ symmetry plane which corresponds to the weaker fracture set. 22% decrease in ε^1 and 9% decrease in δ^1 are observed. For the other symmetry plane XZ which corresponds to the strong fracture set, ε^2 and δ^2 are used and we observe 35% and 5% decrease respectively. We also plot the reflectivity contours and calculate changes in the azimuthal amplitude variation. Figure 2a and 2b compare the reflectivity of the gas and brine saturated sandstones. Brine saturated sands show more azimuthal amplitude variation as AF(30°) increases about 12% after brine substitution.

For higher porosities, we observe that all P-wave moduli and velocities increase more significantly. We observe 30% and 20% decrease in ε^1 and δ^1, 31% and 13% decrease in ε^2 and δ^2. Higher porosity sandstones lead to less azimuthal amplitude variations after brine substitution as we observe 6% decrease in AF(30°).

Those measured experiments show that fluid type has significant influence on elastic moduli, velocities, and anisotropy. For low-porosity sands, the vertical P-wave is insensitive to fractures and fluids for both HTI and orthorhombic media. In

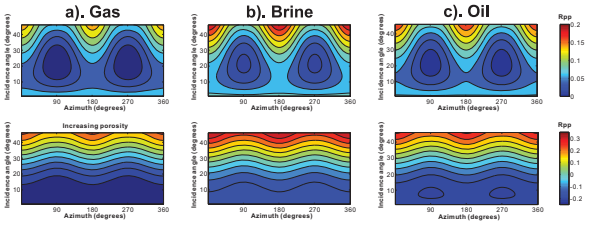

Figure 2. P-wave reflectivity contour for a VTI/Orthorhombic interface as functions of the incidence angle and azimuth. The three columns from left to right are cases for gas, brine and oil respectively. The top row is for the sandstone with low porosity (5%) while the bottom row is for the sandstone with high porosity (25%).

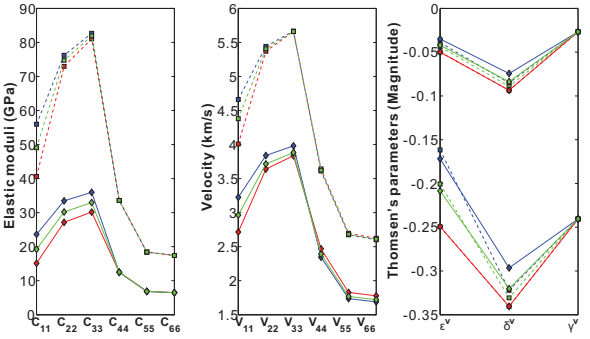

Figure 3. Elastic moduli, velocity and Thomsen's parameter variation with different fluids and porosity combinations. Oil saturation is also calculated for comparison. The colors are coded for different fluid type as gas (red), brine (blue) and oil (green). The dashed line connects the results for low porosity (5%) sandstones while the solid line connects the results for high porosity (25%) sandstones.

this case, we suggest that vertical velocities can be used to estimate the properties of the background isotropic rocks. Sil (2013) uses the vertical velocities from well logs to estimate the properties of the isotropic background and the fracture parameters. However, if the porosity is high, this assumption will not be as accurate as desirable. So this approximation may be more valid for unconventional than conventional reservoirs.

Figure 3 shows the predicted fluid substitution effects for gas sands on elastic moduli, velocities and anisotropy parameters. We add oil saturation in the calculation for comparison. The colors are coded for different fluid type as gas (red), brine (blue) and oil (green). The dashed line connects the results for low porosity sandstones while the solid line connects the results for high porosity sandstones. From the results, we find that brine sands have highest P-wave velocity but lowest S-wave velocity while gas sands are opposite. Also P-wave travelling normal to the fracture planes is more sensitive to fractures and fluid type compared to the parallel direction. All three anisotropy parameters are sensitive to fracture weakness changes. Both $\varepsilon^{1,2}$ and $\delta^{1,2}$ are sensitive to fluid types. For liquid saturated rocks, $\delta^{1,2}$ is also sensitive to porosity. However, $\delta^{1,2}$ is not sensitive to porosity for gas-filled rocks.

CONCLUSIONS

We have derived anisotropic fluid substitution equations for orthorhombic media. The derivation is based on Gassmann's equations and linear slip theory. The results have similar format as the conventional isotropic Gassmann's equations but in terms of stiffness instead of bulk modulus. Gassmann's theory assumes that the shear rigidity is independent of fluids. In many seismic exploration cases, Gassmann's assumptions seem appropriate. We find that brine sands show higher P-wave velocity but lower S-wave velocity compared to gas sands. For low porosity sands, the vertical P-wave is most insensitive to fractures and fluids. The P-wave travelling normal to the fracture planes is most sensitive to fractures and fluid type. All three anisotropy parameters are sensitive to fractures. Both $\varepsilon^{1,2}$ and $\delta^{1,2}$ are sensitive to fluid types. $\delta^{1,2}$ is sensitive to porosity for liquid-saturation, but insensitive to porosity for the case of gas-saturation. Shear-waves splitting ($\gamma^{1,2}$) is only sensitive to fractures weakness. The azimuthal amplitude variation as the result of anisotropy contrast between the interfaces, depends on fluid type and porosity. Significant changes after fluid substitution are observed and we find that gas sands have smaller azimuthal amplitude variation compared to brine sands when the porosity is small. However, with higher porosity, gas sands show more azimuthal amplitude variations. The equations we have derived are straight forward to understand and provide us a useful tool as to quantitatively evaluate the effects of fluid substitution on seismic anisotropy.

ACKNOWLEDGMENTS

This work was supported by AGL (Allied Geophysical Laboratories) at University of Houston and ConocoPhillips. The authors would like to thank Bode Omoboya, Tao Jiang and Jingjing Zong for their helpful discussions. The authors also would like to thank Dr. Colin Sayers and Dr. Leon Thomsen for their online comments on shear-wave dependence on fluid.